Modal Shifts in Acetylcholine Receptor Channel Gating Confer Subunit-Dependent Desensitization

David Naranjo* and Paul Brehm

During the transition from embryonic to adult skeletal muscle, a decreased mean channel open time and accelerated desensitization of nicotinic acetylcholine (ACh) receptors result from the substitution of an ϵ subunit for γ. A single ACh receptor channel of the embryonic type, expressed in *Xenopus* oocytes, interconverts between gating modes of short and long open time, whereas the adult receptor channel resides almost exclusively in the gating mode with short open time. Differences in the fraction of time spent in either gating mode account for the subunit dependence of both receptor open time and desensitization. Therefore, developmental changes in the kinetics of muscle ACh receptors may be imparted through subunit-dependent stabilization of intrinsic gating modes.

Calcium, sodium, potassium, and chloride channels have discrete modes of activity (*1*, *2*); single channel recordings exhibit periods of either high or low activity, presumably reflecting the interconversion between sets of protein configurations. Shifts in gating modes can exert large effects on the size and kinetics of macroscopic membrane currents, as exemplified in the inactivation of voltage-dependent sodium (*3*) and calcium channels (*1*, *4*). The existence of gating modes for ligand-gated ion channels has been revealed by studies on muscle glutamate (*5*) and embryonic and adult forms of ACh receptors (*6*), in which gating modes with different open probabilities were observed. We utilized the *Xenopus* oocyte to express ACh receptors composed of either $\alpha\beta\delta\gamma$ subunits (embryonic type) or $\alpha\beta\delta\epsilon$ subunits (adult type) to determine the effect of subunit composition on desensitization (*7*, *8*) and modal gating (*9*).

In outside-out patches containing several hundred embryonic ACh receptors (*10*), sudden application of 100 μM ACh, a concentration expected to produce near maximal response (*8*, *11*), resulted in macroscopic inward currents that were activated within 5 ms and decayed to half peak value within 100 ms (Fig. 1A). The decay was well described by the sum of two exponential components with time constants that averaged 53.9 ± 14.9 ms (60 ± 12%) and 459 ± 128 ms (*12*) in ten patches (Fig. 1A, inset). The rate of recovery from the desensitized state or states was measured with two-pulse protocols that began with either a long (630 ms) or short (80 ms) conditioning pulse of 100 μM ACh (*13*). For the experiments with the long conditioning pulse (Fig. 1A), the fractional-recovery curves indicated that, similar to the onset of the macroscopic desensitization, recovery from the desensitized state did not proceed as a single time-dependent exponential process (Fig. 1C). The sum of two exponential functions, with fast and slow time constants corresponding to 214 ± 131 ms (42 ± 25%) and 2590 ± 3060 ms, respectively, described the time course of recovery from the desensitized state. That the recovery from the desensitized state was measured in the complete absence of agonist suggests the existence of at least two kinetically distinct desensitized states in the nicotinic ACh receptor (*14*).

The existence of a separable desensitized state with fast recovery was tested with short conditioning pulses 80 ms in duration. Under these conditions, the fractional current recorded during a second application of ACh reflects principally the recovery of the fast component of the desensitization (Fig. 1B) (*15*). The single exponential fit of these data yielded a time constant of 242 ± 13 ms (n = 5 patches). This time constant agrees with the value measured for the fast component of the recovery with the long conditioning-pulse protocol (Fig. 1C), indicating that the desensitization process that has a faster onset also exhibits faster recovery.

Single channel correlates of the two desensitization processes were investigated in patches containing single embryonic or adult receptor proteins (*16*). Complex kinetics were observed for both channel types in response to application of 100 μM ACh. Some traces were characterized by successive short duration openings, others exhibited successive long duration openings, and a few showed transitions between successive openings of long and short duration (arrowheads in Fig. 2A). To determine whether this heterogeneous kinetic behavior corresponded to two or more discrete gating modes, we measured the average open duration, closed duration, and probability of being open for each cluster composed of ten or more openings (*17*). The expected dis-

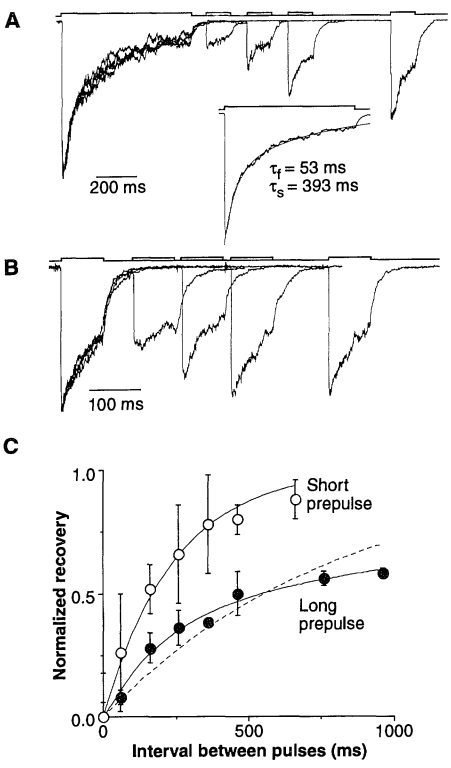

Fig. 1. Time-dependent onset and recovery from the desensitization. (**A**) Current response to the two-pulse protocol with a 630-ms conditioning pulse of 100 μM ACh. The intervals between the conditioning and the test pulses are 70, 270, 470, and 970 ms. Each trace represents a normalized average of 10 to 20 records (*10*). Pipette voltage = −80 mV. (**Inset**) Two-exponential fit to the average of all conditioning records shown in (A). The current trace was fit on the assumption of no steady-state component. Time constants, given in the text, ranged from 33 to 81 ms (fast) and 311 to 731 ms (slow). (**B**) Current records in response to a two-pulse protocol with an 80-ms conditioning pulse. Shown are intervals of 70, 170, 270, and 470 ms. The current response to the test pulse after the shortest time interval lacked the fast desensitizing component that was observed with longer interpulse intervals, further indicating that the fast component does not recover at very short intervals. Each trace corresponds to an average of 10 to 20 records. Pipette voltage = −60 mV. (**C**) Comparison of the recovery of the fractional current that desensitized during the long (630 ms, filled circles) and short (80 ms, open circles) conditioning pulses. For the solid lines, fitting parameters are given in the text. The dashed line indicates the best fit of a single-exponential function, with τ = 801 ± 100 ms, to the recovery data obtained with the long-prepulse protocol. Data were normalized according to the difference between the peak current and the current at the end of the conditioning pulse with the relation $f = 1 - [(f_{test} - 1)/(f_{end} - 1)]$, where f_{end} is the fraction of the current remaining at the end of the conditioning pulse. The values for f_{end} were 0.10 ± 0.05 and 0.5 ± 0.09 for the experiments with long and short protocol, respectively.

Department of Neurobiology and Behavior, State University of New York, Stony Brook, NY 11794.

*To whom correspondence should be addressed.

tribution for the averages of, for example, ten single exponentially distributed open durations is a gamma distribution. Thus, the number of gating modes is reflected in the number of components required in the gamma distribution to fit the histogram of the intracluster open time averages. The sum of three gamma components was required to fit the resultant histogram of pooled intracluster average open times for both embryonic [time constants $\tau_1 = 1.3 \pm 0.1$ ms (32%); $\tau_2 = 3.8 \pm 0.2$ ms (50%); and $\tau_3 = 17.0 \pm 1.1$ ms] and adult [$\tau_1 = 1.2 \pm 0.2$ ms (56%); $\tau_2 = 3.4 \pm 0.6$ ms (38%); and $\tau_3 = 13.5 \pm 3.1$ ms] receptor types (Fig. 2B) (*18*).

Although the sets of time constants for each mode are similar in adult and embryonic receptors, the areas corresponding to each mode differ for the channel types. Openings by the slowest mode (>8 ms) are infrequently observed in the cluster open-time distributions for the adult receptor type. Thus, the embryonic and adult ACh receptors share common gating modes, distinguishable on the basis of open-time differences, which suggests that the differences in open time between adult and embryonic receptors are the consequence of differences in the fractional time spent in a particular mode (*19*). The finding of multiple kinetic modes for both adult and embryonic receptors is in agreement with the results from *Xenopus* myotomal muscle (6) and developing skeletal muscle (*20*).

To test for possible effects of the gating modes on the kinetics of receptor desensitization, we constructed separate ensemble averages for the different modes. Because we could not separate the two shorter open-time modes, we elected to treat all clusters with average open times <8 ms as a single kinetic population (fast mode), different from the long open time population (slow mode) (*21*). Within individual patches, comparison of the ensemble averages for embryonic types indicate a significantly faster decay for short-opening records than the ensemble average for the long-opening records (Fig. 2C, left). When data from the ten experiments on single embryonic receptor channels were pooled, the resultant ensemble average showed two-exponential desensitization kinetics with time constants of 55.8 ± 1.6 ms (61 ± 1%) and 349 ± 9 ms (Fig. 3A), in general agreement with the two time constants of macroscopic current decay measured for patches containing many embryonic-type channels (Fig. 1A, inset).

So that we could eliminate cross-contaminated records containing transitions between fast and slow gating modes (Fig. 2A, arrowheads), records with average open durations between 4 and 16 ms were excluded from ensemble current averages of embryonic receptors (*22*). The two populations of records showed different rates of current decay, with the fast mode measuring 82.8 ± 1.3 ms and the slow mode measuring 283 ± 3 ms (Fig. 3B). The time constant for the fast mode of the embryonic receptor was very similar to the decay constant of 87.2 ± 1.7 ms measured for the fast mode of the adult receptor (Fig. 2C) (*23*). From the fractional steady-state current measured during the ACh application, similar recovery rates from desensitization were estimated for the fast modes of both receptor types (Figs. 2C and 3B). These recovery rates agreed with those obtained independently from the recovery of peak macroscopic current measured by the two-pulse

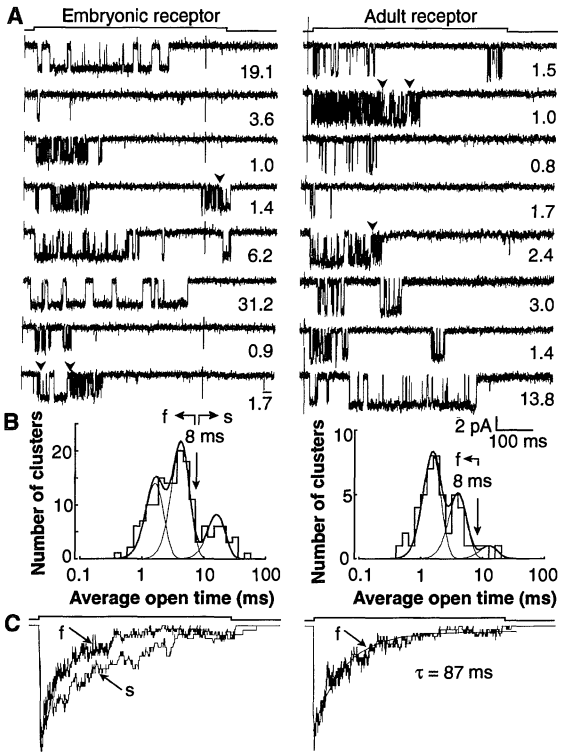

Fig. 2. Modal gating in single embryonic and adult ACh receptors. (**A**) Single channel responses to 530-ms applications of 100 μM ACh. Changes in kinetic mode within records are indicated by arrowheads. The average open time (in milliseconds) is indicated to the right of each trace. The pipette potential was −60 mV. The fast transients at the beginning and near the end of ACh application are electrical artifacts of the solenoid and do not exactly coincide with the onset of ACh application. (**B**) Pooled distribution of the average open times for clusters with ten or more openings separated by closed periods ≤20 ms. Thick lines are maximum-likehood fits (in log time coordinates) of a sum of three gamma distributions (thin lines) for groups of ten events (*18*). (**C**) Ensemble averages constructed from idealized traces with average open times greater than (s) or less than 8 ms (f). An ensemble average for adult receptor data was fitted with a single-exponential function with a steady-state component of 0.05 ± 0.03.

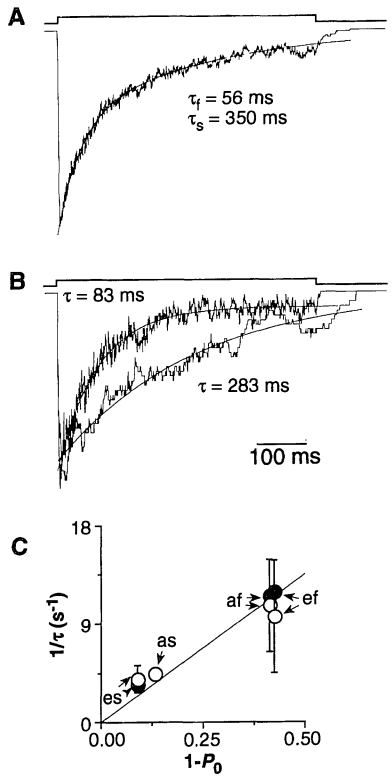

Fig. 3. Macroscopic rates of desensitization for fast and slow gating modes. (**A**) Ensemble averages of 338 idealized single channel records (from ten single channel patches) were summed to obtain the macroscopic rates of desensitization. The solid line is the sum of two exponentials with no steady-state component. (**B**) Ensemble averages constructed for traces having average open times shorter than 4 ms (τ = 83 ms) and average open times longer than 16 ms (τ = 283 ms). Solid lines are fits of single exponential functions to the average records of short open time (with steady-state component of 0.09 ± 0.03) and long open time (with fixed zero steady-state component), respectively. Averages were scaled to match both peak open probabilities, which measured 0.35 and 0.96 for the ensembles of short and long open times, respectively. (**C**) Macroscopic rate of desensitization (filled circles) and average cluster duration (open circles) as a function of the single channel intracluster open probability. Symbols indicate embryonic slow (es), embryonic fast (ef), and adult fast (af) modes. The value for adult slow (as) mode was computed on the basis of only three clusters with average open times longer than 8 ms.

protocol (Fig. 1A), further supporting the idea that the fast component of desensitization corresponds to the fraction of receptors in the fast gating mode (*24*). Consequently, differences in time constants for desensitization of adult and embryonic receptors are attributable to the modal differences in channel gating.

The isolation of the different components of macroscopic desensitization provided estimates of both the onset and recovery rates. The decay phase of the ensemble averages, constructed for the fast mode of the embryonic and adult receptors, was not significantly better fit by the sum of exponentials than by a single exponential. This suggests that, in the presence of 100 μM ACh, receptors in either mode enter a single desensitized state. Because ACh receptors bind two ACh molecules before opening and the probability of being open is nearly maximal at 100 μM ACh (*8, 11, 19*), we assume that, during each agonist application, the receptors are principally in the doubly liganded state (*8, 11*). On the other hand, the linear relationship observed between either the macroscopic rate of desensitization or the cluster duration and the intracluster closed probability ($1 - P_o$) (Fig. 3C) suggests that the transition to the desensitized state occurs mainly from the doubly liganded closed state, as has been proposed for other types of ligand-activated receptor channels (*25*). Thus, a simple scheme can be applied for either the fast mode or the slow mode.

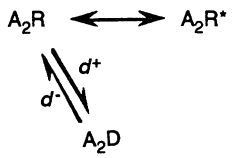

A receptor in the doubly liganded closed state (A_2R) undergoes a conformational transition to either the open state (A_2R^*) or the desensitized state (A_2D), where d^+ and d^- are the microscopic rates of desensitization onset and recovery, respectively. Because the fractional current at the end of the ACh application was less than or equal to one-tenth of the peak for all ensemble averages, $d^+/d^- \geq 9$ for both modes of the embryonic receptor and for the fast mode of the adult type (*26*). These results indicate that the relaxation of the currents is governed almost exclusively by d^+, suggesting identical microscopic onset rates of desensitization ($d^+ = 27\ s^{-1}$) for both kinetic modes of the embryonic receptor and for the fast mode of the adult receptor (slope in Fig. 3C). Thus, the rate of macroscopic desensitization is governed by the closed probability of the primary gating mode of the receptor (*26*).

Because the different modes exhibit large differences in open probability, the variations in the predominance of individual modes between patches may account for the wide variability between patches in desensitization rates and in mean open times reported for the nicotinic receptors of embryonic muscle (*27*). Additionally, the dependence of desensitization rates on the specific agonist (*28*) may in part be explained by the destabilization of a particular gating mode. Finally, the reduction in embryonic receptor channel open time and the time constant for desensitization induced by volatile anesthetics and alcohols (*29*) can be accounted for by a shift to the receptor's fast mode.

Mode switching in channel kinetics appears to be a highly conserved feature among different ion channel types (*1–6*). The ability of channel proteins to exhibit discrete sets of kinetic behavior is best compared with allosteric enzymes that interconvert between configurations that have different catalytic properties (*30*). Thus, intrinsic gating modes for ion channels may be a consequence of a limited number of sets of protein conformations, in which only the residence time in each mode is modulated. The rate of transition between gating modes may be modulated by short-term posttranslational modification (*31*)—as was proposed for the alteration of gating modes in voltage-dependent calcium channels (*4*)—or as directly shown in this study, by longer term structural changes involving subunit substitutions.

REFERENCES AND NOTES

1. P. Hess, J. B. Lansmann, R. W. Tsien, *Nature* **311**, 538 (1984).
2. J. Patlak and M. Ortiz, *J. Gen. Physiol.* **94**, 279 (1989); S. A. Siegelbaum, J. S. Camardo, E. R. Kandel, *Nature* **299**, 413 (1982); O. B. McManus and K. L. Magelby, *J. Physiol. (London)* **402**, 79 (1988); A. L. Blatz and K. L. Magleby, *ibid.* **378**, 141 (1986).
3. J. A. Moorman, G. E. Kirsch, A. M. J. VanDongen, R. H. Joho, A. M. Brown, *Neuron* **4**, 243 (1990); J. Zhou, J. F. Potts, J. S. Trimmer, W. S. Agnew, F. J. Sigworth, *ibid.* **7**, 775 (1991).
4. D. Yue, S. Herzig, E. Marban, *Proc. Natl. Acad. Sci. U.S.A.* **87**, 753 (1990); A. H. Delcour and R. W. Tsien, *Science* **259**, 980 (1993).
5. J. B. Patlak, K. A. F. Gration, P. N. R. Usherwood, *Nature* **278**, 643 (1979).
6. A. Auerbach and C. J. Lingle, *J. Physiol. (London)* **378**, 119 (1986); C. Lingle, D. Maconchie, J. H. Steinbach, *J. Membr. Biol.* **126**, 195 (1992).
7. K. Sumikawa and R. Miledi, *Proc. Natl. Acad. Sci. U.S.A.* **86**, 367 (1989).
8. Compare results from C. Franke, H. Hatt, and J. Dudel [*Pfluegers Arch.* **417**, 509 (1991)] on adult muscle receptors to those of C. Franke, H. Parnas, G. Hovav, and J. Dudel [*Biophys. J.* **64**, 339 (1993)] on embryonic muscle receptors.
9. The high receptor density and diversity on the embryonic muscle [J. Owens and R. Kullberg, *J. Neurosci.* **9**, 1018 (1989)] precludes the formation of patches in which kinetic changes in a single ACh receptor protein with known subunit composition can be studied over time. Utilization of *Xenopus* oocytes to express ACh receptors allowed us to control their subunit composition and density in the patches. Through the manipulation of RNA levels and timing of recording, we could obtain patches ranging from one channel to hundreds of channels (*16*).
10. We prepared RNAs encoding murine αβγδ subunits and rat ε subunits of the ACh receptor by in vitro transcription [R. Kullberg, J. L. Owens, P. Camacho, G. Mandel, P. Brehm, *Proc. Natl. Acad. Sci. U.S.A.* **87**, 2067 (1990)]; they were injected at a final concentration of 25 to 50 ng/μl for each subunit. Methods for oocyte injections and maintenance are given elsewhere [P. Camacho, Y. Liu, G. Mandel, P. Brehm, *J. Neurosci.* **13**, 605 (1993)]. Before patch clamp recording, we mechanically removed the vitelline membranes of oocytes by treatment in a hypertonic solution containing 200 mM potassium aspartate, 10 mM KCl, 10 mM EGTA, and 10 mM Hepes-KOH (pH 7.4) for 10 to 20 min. Electrodes were pulled to an outer diameter of 2 to 3 μm, filled with a solution containing 80 mM KF, 20 mM NaCl, 1 mM $MgCl_2$, 10 mM EGTA, and 10 mM Hepes-KOH and coated with Sigmacote to reduce capacitance. The bath solution contained 115 mM NaCl, 1 mM KCl, 0.2 mM $CaCl_2$, 1 mM $MgCl_2$, and 10 mM Hepes-NaOH (pH 7.4), either with or without 100 μM ACh. To avoid bubble formation inside the tubing, we eliminated the gases dissolved in the solutions by heating to 90°C for 2 min. Outside-out patches were positioned at the point where two streams, one with the bath solution and the other with the ACh-containing solution, converged. Patches were continuously perfused with the bath solution except for brief interruptions by the ACh-containing solution. Rapid solution changes were made by a computer-controlled solenoid valve [R. S. Brett, J. P. Dilger, P. R. Adams, B. Lancaster, *Biophys. J.* **50**, 987 (1986); D. J. Maconochie and D. E. Knight, *Pfluegers Arch.* **414**, 589 (1989)]. The time of the change was judged to be <1 ms, measured on the basis of the time course of the current changes induced by the application of a pulse of a 10% dilution of the extracellular solution to the broken-patch electrode. Currents signals were recorded with an EPC-7 patch-clamp amplifier (List Electronic), filtered at 2 kHz, and digitized at 100-μs intervals. We frequently observed that the size of the macroscopic current gradually decreased during the course of the experiment, taking 5 to 20 min to half decay; however, no change in the kinetics of the macroscopic current decay was observed. Although the rate of the current decay in voltage-clamped oocytes depended on the amount of time after injection, the macroscopic rate of decay in outside-out patches did not.
11. A. Auerbach and C. Lingle, *J. Physiol. (London)* **393**, 437 (1987); S. Sine and J. H. Steinbach, *ibid.* **385**, 325 (1987).
12. All experimental determinations in this report are given as mean ± standard deviation.
13. On termination of the conditioning pulse, the ACh was rapidly removed (within 1 ms) by application of ACh-free external solution. The decay of the ACh-activated current after termination of the pulse could be described by two time constants similar to the average open times for the fast and slow gating modes [Fig. 1, A and B, also see (*10*)]. A second pulse (130 ms in duration) of 100 μM ACh was administered after a variable interval of time (70 to 970 ms) to provide a measure of the time dependence of the recovery process in the absence of ACh. Because desensitization was not complete during the conditioning pulse, we computed the recovery based on the amount of current that desensitized during the conditioning pulse by subtracting the current at the end of the conditioning pulse from the peak current (Fig. 1).
14. B. Sakmann, J. Patlak, E. Neher, *Nature* **286**, 71 (1980); A. Feltz and A. Trautmann, *J. Physiol. (London)* **322**, 257 (1982).
15. According to the two-exponential fitting of the current decay, we estimate that at the end of a 80-ms pulse of 100 μM ACh, 72% of the fast component is already desensitized, compared with only 16% for the slow component.
16. We recorded within 24 hours after RNA injection to optimize the probability of obtaining single

channel patches. A patch was considered to contain a single channel when, after ten successive 530-ms applications of 100 μM ACh, no evidence of simultaneous openings by two or more channels was observed. The average peak open probability (P_o) during a 530-ms pulse was 0.6 within the first 5 ms. Thus, if two identical and independent channels were present, the probability of seeing only single-level openings in n consecutive trials is $[2P_o(1 - P_o)]^n$. At the tenth consecutive trial, this probability is 0.00065, which indicates that a single functional channel is present in the patch.

17. A cluster was defined as ten or more consecutive openings separated by closed periods no longer than 20 ms, a criterion previously used to separate gating modes for ACh receptor channels (*6*). This interval yielded the best separation between modes in the distributions of average open times.
18. The maximum-likelihood method was used to fit gamma distributions. Cumulative and probability-density–function distributions were calculated for one, two, or three gamma components according to D. Colquhoun and B. Sakmann, *J. Physiol. London* **369**, 501 (1985). The negative log of likelihood was minimized with the Gauss-Newton method by a routine in the program AJUSTE [O. Alvarez, A. Villarroel, G. Eisenmann, *Methods Enzymol.* **207**, 816 (1992)].
19. A reduction in the mean channel open time and an increase in the number of openings per cluster have been observed after patch excision in the case of embryonic ACh receptors [M. Covarrubias and J. H. Steinbach, *Pfluegers Arch.* **416**, 385 (1990)]. For all clusters of ten or more openings, we measured a significantly ($P < 0.01$) greater number of openings per cluster in the fast mode (20.5 ± 13.85, $n = 130$) than in the slow mode (14.88 ± 8.82, $n = 30$) (*21*). Thus, the excision effects are consistent with a displacement of the receptor kinetics toward the faster gating modes. The excess openings in the fast mode are consistent with the observed low maximal open probability found in response to the 100 μM ACh applications. Thus, the overall open probability results from the balance between the different gating modes (Fig. 3B).
20. D. Shepherd and P. Brehm, unpublished data.
21. For embryonic receptors, we found sixfold differences in the average open times between fast and slow modes, with 2.8 ± 1.8 ms ($n = 130$ clusters) and 17.1 ± 8.4 ms ($n = 30$ clusters), and intracluster open probabilities of 0.57 ± 0.20 and 0.91 ± 0.05, respectively. However, little difference was observed for the average closed durations, with 2.6 ± 2.0 ms and 1.7 ± 0.8 ms for fast and slow modes, respectively. For the adult receptors, the average open time (2.3 ± 1.6 ms), intracluster open probability ($P_o = 0.58 \pm 0.21$), and average closed time (1.7 ± 2.2 ms) measured for the fast mode (49 of 52 clusters) were similar to those measured for the fast mode of the embryonic receptors.
22. In six out of ten patches containing single embryonic receptor channels, the ensembles constructed for records of short average open time indicate a significantly faster current decay than that observed for records of long average open time. However, the data were pooled because there were often too few ensemble averages from individual experiments to provide reliable fits.
23. Because of the infrequent openings to the slow mode in adult receptors, with an 8-ms cutoff, only a small contamination from this mode is expected in the ensembles made from the records of short open time.
24. The estimated steady-state components for the fast mode of both receptor types, 0.09 ± 0.03 for embryonic and 0.05 ± 0.03 for adult, were not significantly different ($P > 0.68$). These values correspond to an average recovery rate of 2.03 ± 1.33 s^{-1} for the fast modes of both embryonic and adult receptors (*26*). This estimate is in better agreement with the fast component of the macroscopic recovery (4.13 ± 2.86 s^{-1}, $P > 0.52$) than the slow component (0.38 ± 0.45 s^{-1}, $P < 0.23$) obtained from the two-pulse protocol (Fig. 1C). This agreement suggests that the rate-limiting step for the recovery from the desensitized state is the transition away from the desensitized state and not the unbinding of the agonist.
25. J. D. Clements and G. L. Westbrook, *Neuron* **7**, 605 (1991); I. M. Raman and O. Trussell, *ibid.* **9**, 173 (1992); but also see (*8*).
26. The following expression relates open probability to the time constants for macroscopic desensitization (τ): $1/\tau = (1 - P_o)(d^+ + d^-)$. An estimate of d^+ and d^- for each gating mode can be obtained from the fractional current (I) remaining at the end of the response to 530-ms application of the agonist: $I_{end}/I_{peak} \sim d^-/(d^+ + d^-)$.
27. A. J. Gibb, H. Kojima, J. A. Carr, D. Colquhoun, *Proc. R. Soc. London Ser. B* **242**, 108 (1990).
28. J. P. Dilger and Y. Liu, *Pfluegers Arch.* **420**, 479 (1992).
29. J. P. Dilger and R. S. Brett, *Ann. N.Y. Acad. Sci.* **625**, 616 (1991).
30. J. Monod, J. P. Changeux, F. Jacob, *J. Mol. Biol.* **6**, 306 (1963).
31. R. L. Huganir, A. H. Delcour, P. Greengard, G. P. Hess, *Nature* **321**, 774 (1986).
32. We thank D. Shepherd for pointing out the presence of gating modes in mammalian muscle ACh receptors, Y. Liu and J. Dilger for the fast-perfusion method, N. Mendell for suggesting the gamma distribution, and P. Adams, J. Dilger, N. Marrion, and G. Matthews for providing comments on the manuscript. Supported by NIH grant NS18205.

21 December 1992; accepted 26 March 1993

Modulation of Cocaine Self-Administration in the Rat Through D-3 Dopamine Receptors

S. Barak Caine* and George F. Koob

The reinforcing properties of cocaine are probably mediated by the mesocorticolimbic dopamine pathways in the central nervous system, but not all of the dopamine receptor subtypes involved in cocaine's reinforcing actions have been clearly identified. Recently, the D-3 receptor has been cloned, and its distribution in the brain has been found to be relatively restricted to limbic projections of the midbrain dopamine system. The D-3–selective compounds 7-hydroxy-*N,N*-di-*n*-propyl-2-aminotetralin (7-OHDPAT) and quinpirole potently decreased cocaine self-administration in the rat at doses that were not by themselves reinforcing. Moreover, three dopamine receptor agonists had affinities for binding to the D-3 receptor that correlated highly with their relative potencies in decreasing cocaine self-administration. The D-3 receptor may be involved in the reinforcing effects of cocaine and may be a useful target for the development of new pharmacotherapies for cocaine abuse.

It has been hypothesized that cocaine produces its reinforcing properties by inhibiting dopamine reuptake and thereby potentiating dopaminergic neurotransmission (*1*). Lesion studies have shown that cocaine self-administration in the rat depends on an intact mesocorticolimbic dopamine system (*2*). The recent identification of at least five dopamine receptor subtypes (*3–5*) with distinct molecular and pharmacological properties, as well as different anatomical distributions, provides a means for the evaluation of the relative contribution of these subtypes in cocaine reinforcement.

The paucity of highly selective ligands for dopamine receptor subtypes makes the unambiguous determination of the function of these subtypes in cocaine self-administration difficult (*6*). However, the recently developed D-3–selective compound 7-OHDPAT binds to D-3 receptors with an affinity of <1 nM and has a lower (weaker) affinity for other subtypes (about 10^2-, 10^3-, and 10^4-fold lower affinity for D-2, D-4, and D-1 receptors, respectively) (*7*). Quinpirole has approximately equal affinity for D-3 and D-4 receptors and has about 100-fold and 3000-fold lower affinity for D-2 and D-1 receptors, respectively (*7, 8*). Apomorphine has high affinity for D-4 receptors, about 10-fold lower affinity for D-3 and D-2 receptors, and 100-fold lower affinity for D-1 receptors (*7, 8*). Using these three dopamine agonists, we investigated the ability of D-3 receptors to modulate cocaine self-administration in the rat.

Male Wistar rats were implanted with long-term jugular catheters and trained to self-administer cocaine intravenously in daily 3-hour sessions (*9*). Once baseline rates of cocaine self-administration were established, various doses of dopamine agonists were combined with cocaine in the self-administration syringe (*9*). All of the dopamine agonists, when self-administered in combination with cocaine, reduced cocaine intake by producing an increase in the interval between injections without disrupting self-administration (Fig. 1). This is interpreted as an enhancement of cocaine's reinforcing effects because an increase in the dose of cocaine produces the same effect (*10*). The relative potencies of the various agonists to decrease cocaine self-administration were calculated from

Department of Neuropharmacology, Scripps Research Institute, La Jolla, CA 92037.

*To whom correspondence should be addressed.